Biosensors and Bioelectronics 127 (2019) 229–235

Contents lists available at ScienceDirect

Biosensors and Bioelectronics

journal homepage: www.elsevier.com/locate/bios

# Micropatterning of porous silicon Bragg reflectors with poly(ethylene glycol) to fabricate cell microarrays: Towards single cell sensing

Ranjana Piya[a,b], Ying Zhu[a,b], Alexander H. Soeriyadi[a], Saimon M. Silva[a], Peter J. Reece[b,*], J. Justin Gooding[a,*]

[a] School of Chemistry, Australian Centre for NanoMedicine and the ARC Centre of Excellence in Convergent Bio-Nano Science and Technology, The University of New South Wales, Sydney 2052, Australia
[b] School of Physics, The University of New South Wales, Sydney 2052, Australia

ARTICLE INFO

*Keywords:*
Porous silicon (PSi)
Cell patterning
Cell lysis
Label-free biosensing
Poly(ethylene glycol) (PEG) hydrogel

ABSTRACT

The work presented here describes the development of an optical label-free biosensor based on a porous silicon (PSi) Bragg reflector to study heterogeneity in single cells. Photolithographic patterning of a poly(ethylene glycol) (PEG) hydrogel with a photoinitiator was employed on RGD peptide-modified PSi to create micropatterns with cell adhesive and cell repellent areas. Macrophage J774 cells were incubated to form cell microarrays and single cell arrays. Moreover, cells on the microarrays were lysed osmotically with Milli-Q™ water and the infiltration of cell lysate into the porous matrix was monitored by measuring the red shift in the reflectivity. On average, the magnitude of red shift increased with the increase in the number of cells on the micropatterns. The red shift from the spots with single cells varied from spot to spot emphasizing the heterogeneous nature of the individual cells.

## 1. Introduction

The ability to position single or multiple cells at predefined locations, also known as cell patterning, is a technique enabling the study of fundamental aspects of cell biology such as cell-cell interactions, interaction of cells with their microenvironment and reaction of cells to external stimuli (Chen et al., 1998; Raghavan and Chen, 2004; Lamponi et al., 2009; Yarmush and King, 2009). Many varieties of micropatterning techniques can be used for the generation of cell microarrays including spotting, photolithography, soft lithography and microfluidic devices (Zhang et al., 1999; Yap and Zhang, 2007; Ceriotti et al., 2009). Among these techniques, micropatterning of photopolymerizable hydrogels using photolithography has received growing attention as it enables the formation of precise 3D microstructures in simple steps (Revzin et al., 2001; Yanagawa et al., 2016). Hydrogels based on poly(ethylene glycol) are commonly used in cell-based assays as they are both nonfouling and biocompatible in complex environments (Bjugstad et al., 2008; Kim et al., 2009; Bjugstad et al., 2010). PEG with multiple polymerizable end groups with a photoinitiator can form cell or protein repelling hydrogel microstructures using UV initiated free radical polymerization (Revzin et al., 2001; Ekblad et al., 2008; Bae et al., 2010; Yeh et al., 2016). Such hydrogel microstructures can be exploited for cell patterning to study different aspects of cell biology including detection of cell secreted proteases (Shin et al., 2012; Son et al., 2013), cytokines (Zhu et al., 2008, 2009; Yan and Revzin, 2012), cell metabolites (Yan et al., 2009) and for cell capture and release (Shin et al., 2011; Shin et al., 2014). PEG hydrogel patterning has been extensively conducted on flat surfaces like glass and silicon (Koh et al., 2002; Revzin et al., 2003) with some examples reported for porous substrates like nanoporous alumina (Lee et al., 2011). The advantage of using a porous substrate is that the hydrogel crosslinking can take place inside the porous matrix, thus firmly fixing the hydrogel micropatterns to the substrate.

Porous silicon (PSi) is a versatile material for cell-based assays due to its biocompatibility (Chin et al., 2001; Low et al., 2006; Low et al., 2009), tunable optical properties and label-free optical biosensing (Schwartz et al., 2006; Kilian et al., 2009; Guan et al., 2011; Gupta et al., 2015). Moreover, PSi is compatible with microfabrication techniques, which makes it an ideal platform for the formation of cell microarrays. PSi can be fabricated by electrochemically etching single crystalline silicon wafers and optical properties tuned to reflect light at particular wavelengths. The sensing of PSi relies on the change in the position of the reflectivity peak in response to the exchange of materials with different refractive indices into or from the pores. This mode of sensing makes PSi biosensors a possible label-free platform to study response of cells to external stimuli. Although there are various reports on micropatterning of PSi to promote selective cellular attachment to

* Corresponding authors.
*E-mail addresses:* p.reece@unsw.edu.au (P.J. Reece), justin.gooding@unsw.edu.au (J.J. Gooding).

https://doi.org/10.1016/j.bios.2018.12.001
Received 28 October 2018; Received in revised form 21 November 2018; Accepted 2 December 2018
Available online 07 December 2018
0956-5663/ 

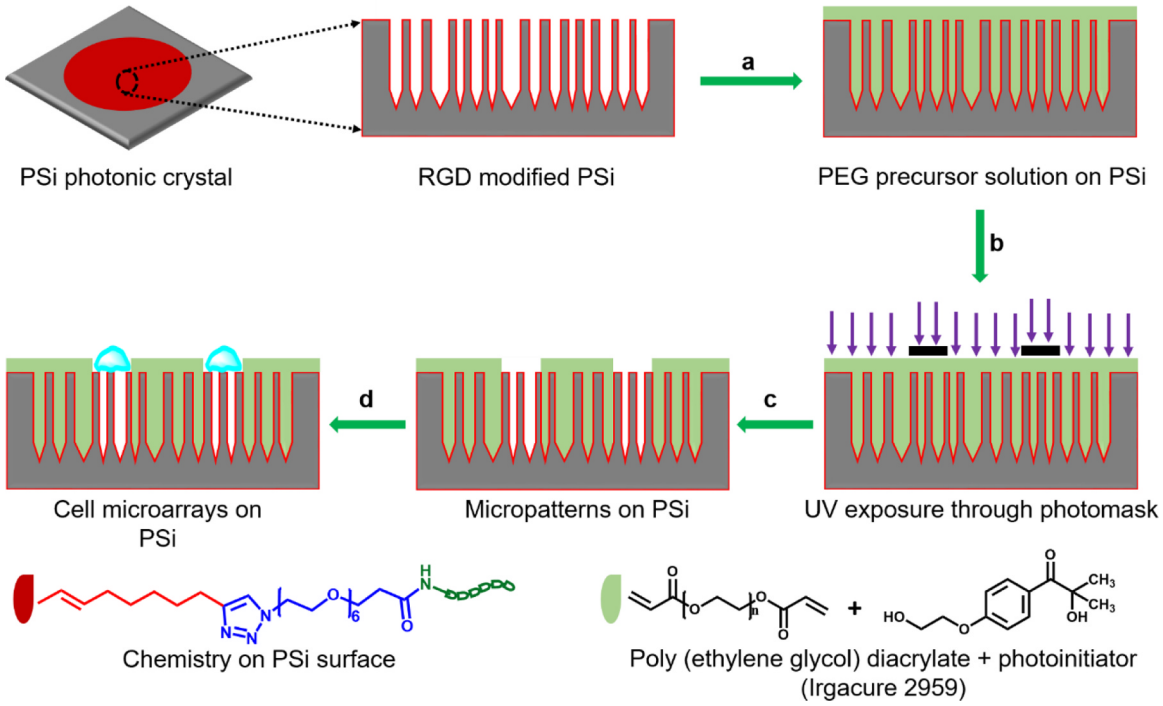


**Fig. 1.** Top view and cross-section scheme depicting the photolithographic strategy to form PEG hydrogel micropatterns and cell microarray on PSi. (a) PEG precursor solution containing PEGDA and photoinitiator (Irgacure 2959) was dropped on RGD peptide-modified PSi, (b) a glass coverslip was placed on top of PSi and the substrate irradiated with UV light through a chrome-patterned photomask in a mask aligner, (c) exposed substrate was developed with water/ethanol mixture to wash unexposed PEG solution thus forming micropatterns with exposed RGD peptide and (d) J774 macrophage cells were incubated with PEG hydrogel patterned PSi to form cell microarrays.

defined locations (Khung et al., 2006; Flavel et al., 2011; Sweetman et al., 2011; Sweetman et al., 2012; Dalilottojari et al., 2016) in order to control the number of cells being studied, the potential for PSi as a label-free optical biosensor to study cellular behaviour in cell microarrays has not been explored until now.

In this paper, we demonstrate the fabrication of single and multi-cell microarrays on PSi photonic structures using PEG hydrogel patterning. Also, we show that label-free optical sensing of single cells is possible using a cell lysis assay. To form cell microarrays, the PSi was first modified with the arginine-glycine-aspartic acid (RGD) peptide for selective cell attachment to defined positions. Then photolithographic PEG hydrogel patterning was performed using a PEG precursor solution containing poly(ethylene glycol) diacrylate (PEGDA) and photoinitiator (Irgacure 2959). The area of PSi with exposed RGD promotes selective cell attachment while the area with PEG hydrogel prevents non-specific cell adsorption. Single and multi-cell microarrays were fabricated by incubating J774 macrophage cells on the patterned PSi surface. To demonstrate the utility of PSi as an optical biosensor in cell-based assays, shifts in optical reflectivity were monitored after osmotic lysis of the cells on microarrays followed by lysate infiltration of the porous matrix. Cell lysis was also confirmed by monitoring the leakage of stain from cells using a fluorescence microscope.

## 2. Materials and methods

Details on chemicals, materials, apparatus and experiment procedures used in this work can be found in the Supplementary Information.

## 3. Results and discussion

### 3.1. Surface modification of PSi Bragg reflectors

To make PSi Bragg reflector surfaces amenable for the selective attachment of cells at precise locations, the freshly etched PSi Bragg reflector samples were first modified with multiple surface chemistry modification steps as shown in Fig. S2a. Reflectivity spectra were collected after each modification step as a means to characterize the attachment of molecular components (Fig. S2b). When freshly etched PSi was hydrosilylated with 1,8-nonadiyne, Si-H bonds were replaced by robust Si-C bonds forming an organic monolayer on PSi that prevents PSi surface degradation in biological media. Since the air-silicon interface was replaced by an organic-silicon interface, there was an associated increase in the average refractive index of PSi, red shifting the reflectivity peak position. Hydrosilylation of the dialkyne in this case resulted in a red shift of 41.5 nm (s = 1.0 nm, n = 35) where s is the standard deviation and n is the number of spots measured. Further modification of the alkyne-terminated PSi with carboxyl group-terminated azide-containing hexaethylene glycol-based linker ($EO_6$) moieties *via* the archetypal click reaction, the Huisgen-1,3-dipolar cycloaddition, resulted in another red shift of 7.4 nm (s = 1.0 nm, n = 35). This surface was further modified to promote cell adhesion with the RGD peptide using EDC/NHS chemistry. Since the RGD peptide is short, this only resulted in a red shift of 1.8 nm (s = 1.0 nm, n = 35). Each surface modification step was also confirmed by surface XPS measurement (Fig. S3). The XPS survey spectra and narrow scans of Si 2p and C 1 s on the PSi Bragg reflector passivated with 1,8-nonadiyne are presented in Fig. S3a-c. Survey spectra show the presence of expected elements such as Si, C and O on the surface. The peak at binding energy 285 eV (Fig. S3c) is indicative of carbon-carbon bonds (C-C) from the functionalized alkyne layer. Survey spectra of the click functionalized PSi Bragg reflector show the presence of nitrogen (Fig. S3d) confirming the successful derivatization of alkyne functionalized PSi with azide containing $EO_6$ moieties (Ciampi et al., 2007). The narrow scan of C 1 s (Fig. S3f) shows additional peaks at binding energies 286.8 eV, indicative of C-O, and 289.5 eV indicative of O-C = O. The high resolution N 1 s data (Fig. S3e) shows two peaks centered at binding energies 400.5 eV and 402.0 eV, indicative of chemically distinct nitrogen. This strongly suggests the formation of triazole moiety and supports successful modification of the

PSi Bragg reflector surface with an azide species. An increase in the intensity of the nitrogen peak at binding energy 400.5 eV (Fig. S3h) after peptide attachment is attributed to the additional nitrogen containing peptide bonds. Also, there is a significant increase in the intensity of O-C = O peak at 289.5 eV, attributed to the peptide carboxylic acid group.

### 3.2. PEG hydrogel patterning on PSi Bragg reflectors

The scheme depicting PEG hydrogel patterning on the RGD peptide-modified PSi Bragg reflector is shown in Fig. 1. In a typical experiment, a PEG precursor solution containing PEGDA and a photoinitiator (Irgacure 2959) was dropped onto the RGD peptide-modified PSi surface and a glass coverslip placed on top. The glass coverslip helped to homogeneously distribute the precursor solution over the surface and prevent direct contact between the photomask and substrate. Subsequently the PSi substrate was exposed to UV light for 20 s through the photomask in the MA6 mask aligner. The PEG precursor solution behaved as a negative photoresist. Upon precursor solution exposure to UV light, the photoinitiator dissociates into free radicals that attack the C = C of the monomer and initiate free radical polymerization. In this manner, the precursor solution in the exposed region was crosslinked to form a hydrogel *via* radical chain polymerization (Fisher et al., 2001; Tan et al., 2008). The precursor solution from the unexposed regions was washed away with a water/ethanol mixture. Equation (i) demonstrates the PEG hydrogel formation process from the PEG precursor solution.

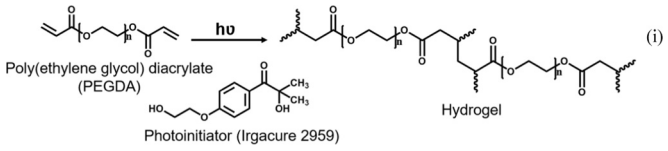


### 3.3. Formation of micropatterns and cell microarrays on PSi Bragg reflectors

The bright field images in Fig. 2a show PEG hydrogel micropatterns formed on PSi with different feature sizes. The dimensions of the micropatterns were controlled using a photomask with different pattern size. The pattern size of the mask and the pattern formed on the surface can differ slightly depending upon slight over or underexposure of the substrate and due to imperfect contact between substrate and mask. With a pattern size of 65 μm on the photomask, the pattern size formed on PSi was 65.1 μm (s = 1.8 μm, n = 100). Similarly with the mask pattern size of 50 μm and 20 μm, the pattern size formed was 49.6 μm (s = 2.1 μm, n = 100) and 20.1 μm (s = 1.5 μm, n = 100) respectively. Within the circular regions, the RGD peptide surface is exposed promoting cell attachment within the circle (D'Souza et al., 1991; Bellis, 2011). The RGD peptide is found in extracellular matrix proteins, namely fibronectin, and is recognized by integrin cell surface receptors (Ruoslahti and Pierschbacher, 1987; Ruoslahti, 1996). Outside the circle the antifouling PEG hydrogel restricts cell attachment (Ekblad et al., 2008; Yeh et al., 2016). Thus the micropatterns formed on PSi with PEG hydrogel patterning have a potential for cell microarray formation.

For the formation of cell microarrays and single cell arrays, micropatterned PSi surfaces with different circle diameters were incubated with J774 macrophage cells for 6 h. Since the average size of J774 macrophage cells is 20 μm, we used 20 μm patterns for the fabrication of single cell arrays. After 6 h, surfaces were washed with growth media 3 times to remove unbound or loosely bound cells on the surface. Cells were then stained with live/dead stain to check the viability of cells on the micropatterns. Fig. 2b shows the fluorescence images of cell microarrays formed on PEG hydrogel micropatterns with different circle diameters. From the images, it is shown that cells adhered only to the RGD peptide-modified area in PEG hydrogel patterned PSi. The green fluorescence is due to the enzymatic conversion of cell-permeant nonfluorescent calcein AM (live component in live/dead stain) to intensely fluorescent calcein in live cells. Ethidium homodimer-1 (dead component in live/dead stain) only enters cells with damaged membranes, expressing very intense red fluorescence by interacting with nucleic acid. All the cells expressed an intense uniform green fluorescence indicating that the surfaces are cell compatible. Cell occupancy % was calculated for different pattern sizes at the same cell seeding density ($1 \times 10^6$ cells/mL). For the larger sized micropatterns (65 μm and 50 μm circle diameter), no empty spots were observed yielding 100% cell occupancy but in case of smaller micropatterns (20 μm circle diameter), cell occupancy % was less (59.4%). Of the total number of occupied spots in the 20 μm arrays, 65% were occupied by a single cell.

Fig. 2c presents the actual number of cells adhered on the different patterns, demonstrating control over the number of cells per pattern by using different pattern size.

### 3.4. Cell lysis on PSi cell microarrays

To demonstrate the use of PSi Bragg reflectors as optical biosensors in cell-based assays for the analysis and to discriminate between few and/or single cells, cells on the microarrays were lysed chemically using a lysis buffer Triton X-100 (0.1%) in PBS. When the cells are lysed, the cell membrane is ruptured and the released contents (cell lysate) infiltrate the porous matrix. Since the lysate contains proteins, ingress into the porous matrix causes an increase in the average refractive index of PSi and a red shift of the reflectivity spectrum maxima. Before lysis, cells were first stained with calcein AM. When the cells are lysed, there is a leakage of calcein from inside the cells due to cell membrane rupture (Fig. 3b) that leads to a decrease in fluorescence intensity. To confirm that cells are actually lysed with lysis buffer and to rule out photobleaching, the fluorescence intensity of cells exposed to only PBS was measured (Fig. S4e). We found that the mean fluorescence intensity of cells exposed to lysis buffer dropped down to background in 6 min whereas the mean fluorescence intensity from spots containing non-lysed cells remained similar upon longer exposure to light when in PBS without Triton X-100 (Fig. S5).

After confirming that cells can be efficiently lysed on the micropatterns with a lysis buffer, we collected the reflectivity spectra from the micropatterns with cells + lysis buffer as well as no cells + lysis buffer. We found that the spots without cells exhibited a small red shift due to surfactants present in the lysis buffer adsorbing to the pore walls and increasing the average refractive index of PSi in those spots. Such red shift from the spots without cells is undesirable especially when the goal is to detect very small changes in the amount of material released from cell into the pores. As such, to avoid any undesirable red shift caused by lysis buffer, we next explored the osmotic lysis of cells using Milli-Q™ water. Milli-Q™ water does not cause any undesirable red shifts. J774 macrophage cells were first incubated on PEG hydrogel patterned PSi surface for 6 h in culture media. Then the culture media was replaced with Milli-Q™ water after removing the unbound cells by washing with culture media. When the culture media was replaced with Milli-Q™ water, the osmotic imbalance inside and outside the cells causes excess water to move into the cells. As a result, the volume of the cell increased and reached the point where the volume exceeded the membrane's capacity, thus causing the membrane of the cell to rupture and their contents to enter the pores of the PSi. Some residual cell fragments can be observed after cell lysis (Fig. S6b). Due to contents of the cells infiltrating into the pores there is an increase in the average refractive index of PSi, thus causing a red shift in the reflectivity peak.

For single cell lysis, the cells were cultured on the PEG hydrogel

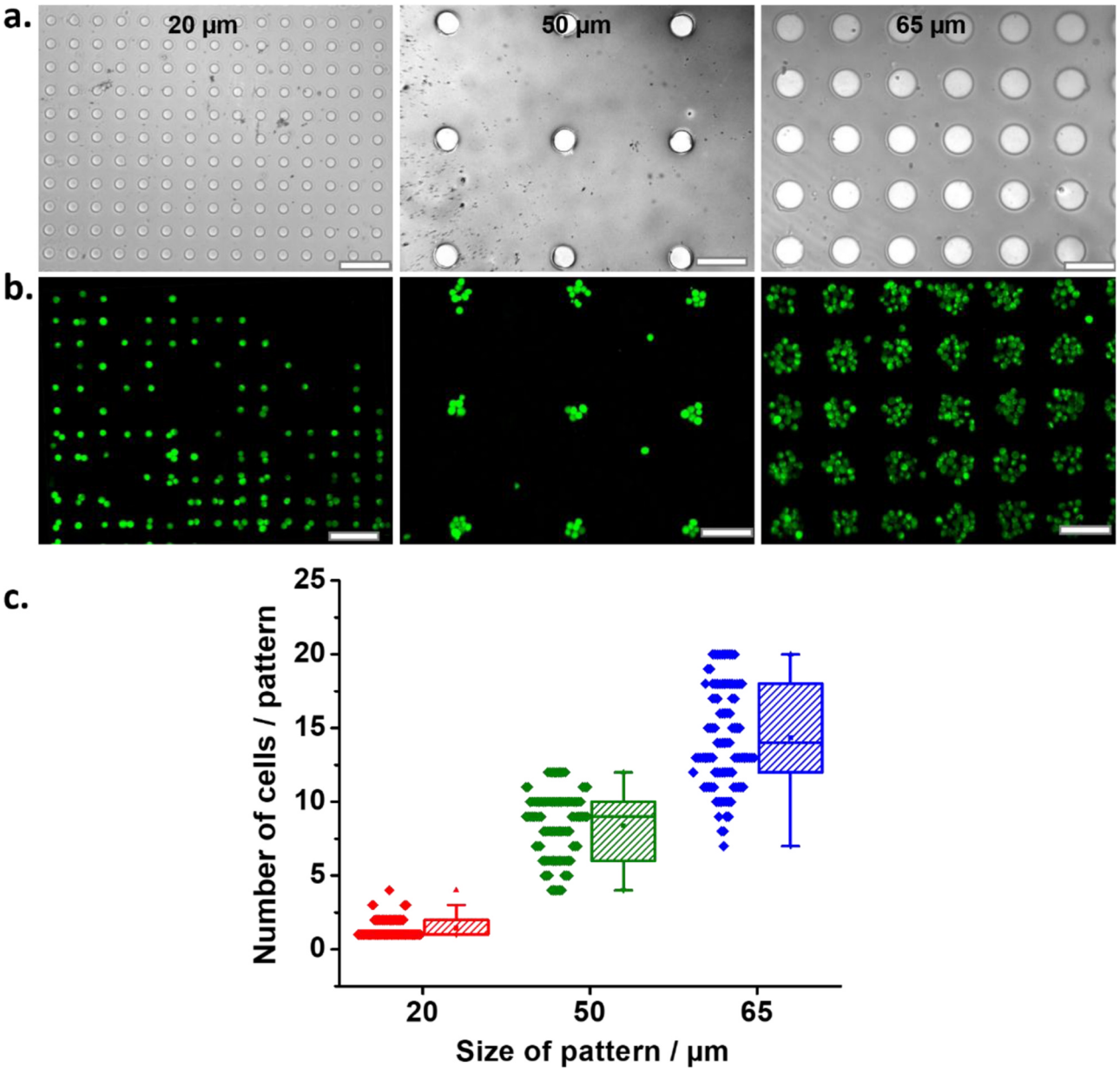


**Fig. 2.** (a) Bright field images of micropatterns formed on PSi with circle diameters 20 µm, 50 µm and 65 µm. (b) Fluorescence images of live/dead stained J774 macrophage cells on the corresponding micropatterns showing the formation of cell microarrays and single cell arrays and (c) the plot showing number of cells adhered on spots with different diameters. The size of micropatterns can be controlled by using a photomask with different pattern size. The circular region has exposed RGD peptides for cell attachment whereas outside the circle has antifouling PEG hydrogel to prevent attachment of cells. The green fluorescence is due to the enzymatic conversion of cell-permeant nonfluorescent calcein AM (live component in live/dead stain) to intensely fluorescent calcein in live cells (scale bar 100 µm).

patterned PSi sample with a circle diameter of 20 µm. Reflectivity measurements were performed after 6 h of Milli-Q™ water exposure. As a control, reflectivity was also collected from the sample with cells left in the culture media for 6 h. Fig. 4a presents the plot of reflectivity peak shift for test (cells exposed to water) and control (cells left in culture media) samples. We observed that the spots in the sample with cells left in culture media for 6 h showed almost no change in reflectivity or a minor blue shift presumably due to oxidation of the underlying silicon (Böcking et al., 2008) whereas there is a noticeable red shift in most of the spots in the test sample exposed to Milli-Q™ water. This demonstrates the infiltration of cell contents into the porous matrix after rupture which increases the average refractive index of PSi. Within Fig. 4b is presented the statistical analysis of the optical shift based on Student's *t*-test. There is a significant difference in the red shift obtained from the spots with lysed cells compared to non-lysed cells. In Fig. 4c is depicted the red shift obtained from individual spots in 20 µm patterns occupied by one, two and three lysed cells. From the plot there is a linear increase in the average red shift as the number of cells lysed increases. Most of the spots with lysed single cells have red shift ranging from 0.6 to 1.4 nm (n = 65). Seen in Fig. 4d is the histogram showing red shift obtained from individual spots upon which lysed single cells were located. The histograms show significant single cell response heterogeneity. At this stage it cannot be determined whether this variation in red shift is due to heterogeneity within individual cells or from how the cells were ruptured and variation in the amount of material that entered the pores.

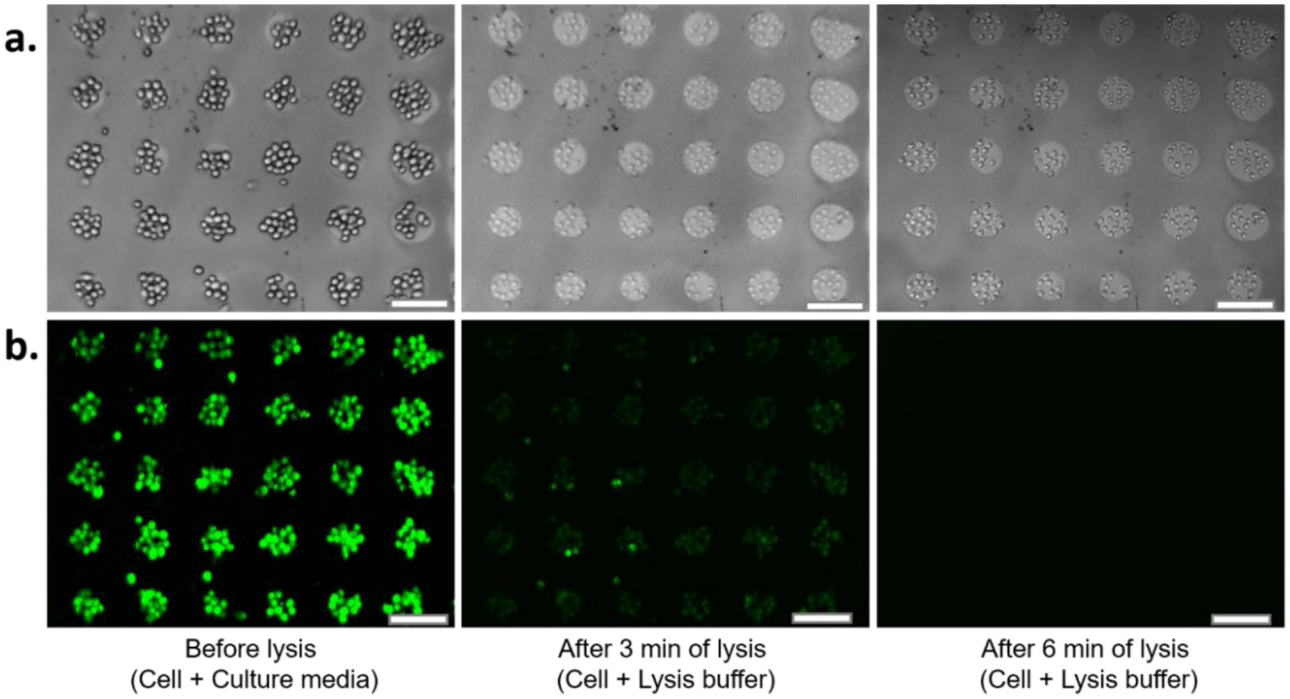


**Fig. 3.** (a) Bright field and (b) fluorescence images of J774 macrophage cells on 65 μm pattern before and after lysis. Cells were stained with calcein AM. When the cells are lysed, pores are created on the cell membrane thus causing the leakage of calcein from the cells. Thus the fluorescence intensity started to decrease due to the calcein leakage. Cells still on the micropatterns after lysis can be seen from BF images. Scale bar 100 μm.

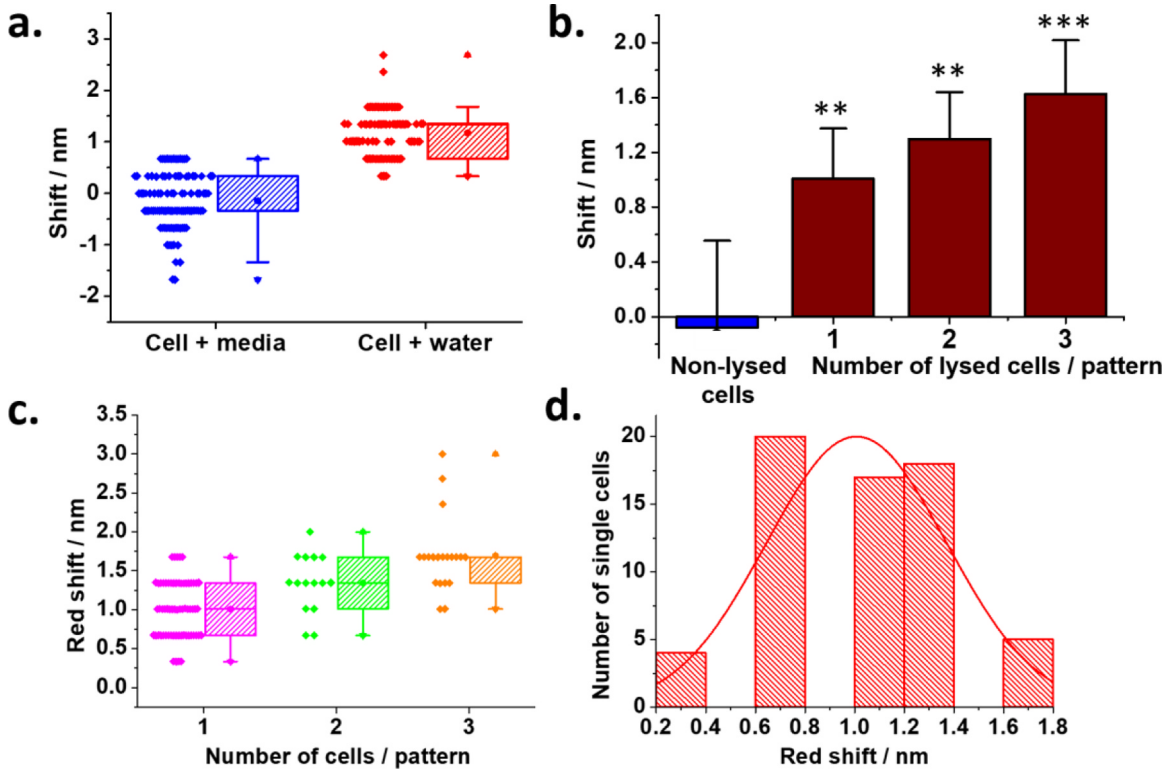


**Fig. 4.** (a) Plot of optical shifts obtained from the spots of test sample (cell + water) and control sample (cell + culture media) with 20 μm circle diameter. There is a noticeable red shift from most of the spots of the sample exposed to water which is attributed to the infiltration of cellular contents into the porous matrix due to bursting of cells. On the other hand, most of the spots of the sample left in culture media have seen some blue shift. (b) Statistical analysis of red shift obtained from non-lysed cells (cell + media) and lysed cells (cell + water). Statistical significance was determined by Student's *t*-test. The bars with * * and * ** indicate a statistical significance difference $p < 0.01$ and $p < 0.001$ respectively. Error bar is standard deviation. (c) Plot of optical shift obtained from individual spots with different number of cells (data analyzed from two different surfaces, n = 2) which shows that the average red shift increases with an increase in the number of cells. (d) Histograms showing red shift from spots with single cells. Most of the spots with a single cell have red shifts ranging from 0.6 to 1.4 nm.

## 4. Conclusion

In summary, the work presented in this paper demonstrates the potential of using a PSi optical biosensor for label-free detection of biological events with single cell-resolution. PEG hydrogel patterned PSi Bragg reflectors were shown to be compatible for the formation of cell microarrays and single cell arrays. In this proof of concept study the cells adhered to individual elements of the array using the nonselective cell adhesive peptide RGD. However, we have previously shown on silicon surfaces that selectivity for one cell type over another can be achieved using antibodies (Guan et al., 2014; Parker et al., 2018). It was also demonstrated that the number of cells on the spots can be controlled by fabricating micropatterns of different diameter. To demonstrate the utility of PSi Bragg reflector as a label-free optical biosensor for monitoring single cell activities, cells on the micropatterns were lysed chemically and osmotically with the ingress of cell lysate into the porous matrix monitored via red shift of the reflectivity spectrum. Significant difference in the red shift from spots with lysed cells in comparison to non-lysed cells was observed, highlighting the sensitivity of the PSi optical biosensor in monitoring cellular activities at single-cell resolution. Cell lysis was also confirmed by measuring the decrease in mean fluorescence intensity from chemically-lysed cells.

The ability to monitor single cell response to specific stimuli has broad implications in studying cellular heterogeneity. At this stage the results demonstrate that sufficient material is released from cells for PSi based cell arrays to explore cell heterogeneity. However, as stated above, at this stage it is not 100% certain whether the heterogeneity in single cell response is due to cell content heterogeneity or variance in cell rupture. This can be elucidated from methods with more controlled cell content release properties. For example, with macrophage cells we have previously shown that matrix metalloproteinase release can be stimulated using lipopolysaccharide (Kilian et al., 2009). Such a strategy has yet to be explored at the single cell level but is more suitable in exploring single cell heterogeneity, especially as the release of enzymes engenders the sensing system with an inbuilt amplification scheme, arising from the fact that each enzyme molecule can react with many substrate molecules inside the PSi pores. As such, the system developed in the present study can be easily extended to study different biological events such as detecting enzymes, cytokines and metabolites released by single cells which could have great importance in studying cellular heterogeneity.

## Acknowledgements

We acknowledge the generous financial support from the Australian Research Council through the Centre of Excellence in Convergent Bio-Nano Science and Technology (CE140100036), the ARC Australian Laureate fellowship (FL150100060) for J.J.G. and the NHMRC Early Career Fellowship (1092005) to A.H.S.

## Appendix A. Supplementary material

Supplementary data associated with this article can be found in the online version at doi:10.1016/j.bios.2018.12.001.

## References

Bae, M., Divan, R., Suthar, K.J., Mancini, D.C., Gemeinhart, R.A., 2010. Fabrication of poly(ethylene glycol) hydrogel structures for pharmaceutical applications using electron beam and optical lithography. J. Vac. Sci. Technol. B Microelectron. Nanometer Struct. Process Meas. Phenom. 28 (6), C6P24–C26P29.

Bellis, S.L., 2011. Advantages of RGD peptides for directing cell association with biomaterials. Biomaterials 32 (18), 4205–4210.

Bjugstad, K.B., Lampe, K., Kern, D.S., Mahoney, M., 2010. Biocompatibility of poly (ethylene glycol)-based hydrogels in the brain: an analysis of the glial response across space and time. J. Biomed. Mater. Res A 95 (1), 79–91.

Bjugstad, K.B., Redmond Jr., D.E., Lampe, K.J., Kern, D.S., Sladek Jr., J.R., Mahoney, M.J., 2008. Biocompatibility of PEG-based hydrogels in primate brain. Cell Transplant. 17 (4), 409–415.

Böcking, T., Kilian, K.A., Gaus, K., Gooding, J.J., 2008. Modifying porous silicon with self-assembled monolayers for biomedical applications: the influence of surface coverage on stability and biomolecule coupling. Adv. Funct. Mater. 18 (23), 3827–3833.

Ceriotti, L., Buzanska, L., Rauscher, H., Mannelli, I., Sirghi, L., Gilliland, D., Hasiwa, M., Bretagnol, F., Zychowicz, M., Ruiz, A., Bremer, S., Coecke, S., Colpo, P., Rossi, F., 2009. Fabrication and characterization of protein arrays for stem cell patterning. Soft Matter 5 (7), 1406–1416.

Chen, C.S., Mrksich, M., Huang, S., Whitesides, G.M., Ingber, D.E., 1998. Micropatterned surfaces for control of cell shape, position, and function. Biotechnol. Prog. 14 (3), 356–363.

Chin, V., Collins, B.E., Sailor, M.J., Bhatia, S.N., 2001. Compatibility of primary hepatocytes with oxidized nanoporous silicon. Adv. Mater. 13 (24), 1877–1880.

Ciampi, S., Böcking, T., Kilian, K.A., James, M., Harper, J.B., Gooding, J.J., 2007. Functionalization of acetylene-terminated monolayers on Si(100) surfaces: a click chemistry approach. Langmuir 23 (18), 9320–9329.

D'Souza, S.E., Ginsberg, M.H., Plow, E.F., 1991. Arginyl-glycyl-aspartic acid (RGD): a cell adhesion motif. Trends Biochem Sci. 16 (7), 246–250.

Dalilottojari, A., Delalat, B., Harding, F.J., Cockshell, M.P., Bonder, C.S., Voelcker, N.H., 2016. Porous silicon-based cell microarrays: optimizing human endothelial cell-material surface interactions and bioactive release. Biomacromolecules 17 (11), 3724–3731.

Ekblad, T., Bergström, G., Ederth, T., Conlan, S.L., Mutton, R., Clare, A.S., Wang, S., Liu, Y., Zhao, Q., D'Souza, F., Donnelly, G.T., Willemsen, P.R., Pettitt, M.E., Callow, M.E., Callow, J.A., Liedberg, B., 2008. Poly(ethylene glycol)-containing hydrogel surfaces for antifouling applications in marine and freshwater environments. Biomacromolecules 9 (10), 2775–2783.

Fisher, J.P., Dean, D., Engel, P.S., Mikos, A.G., 2001. Photoinitiated polymerization of biomaterials. Annu. Rev. Mater. Res. 31 (1), 171–181.

Flavel, B.S., Sweetman, M.J., Shearer, C.J., Shapter, J.G., Voelcker, N.H., 2011. Micropatterned arrays of porous silicon: toward sensory biointerfaces. Acs Appl. Mater. Interfaces 3 (7), 2463–2471.

Guan, B., Magenau, A., Ciampi, S., Gaus, K., Reece, P.J., Gooding, J.J., 2014. Antibody modified porous silicon microparticles for the selective capture of cells. Bioconjugate Chem. 25 (7), 1282–1289.

Guan, B., Magenau, A., Kilian, K.A., Ciampi, S., Gaus, K., Reece, P.J., Gooding, J.J., 2011. Mesoporous silicon photonic crystal microparticles: towards single-cell optical biosensors. Faraday Discuss. 149, 301–317.

Gupta, B., Mai, K., Lowe, S.B., Wakefield, D., Di Girolamo, N., Gaus, K., Reece, P.J., Gooding, J.J., 2015. Ultrasensitive and specific measurement of protease activity using functionalized photonic crystals. Anal. Chem. 87 (19), 9946–9953.

Khung, Y.-L., Graney, S.D., Voelcker, N.H., 2006. Micropatterning of porous silicon films by direct laser writing. Biotechnol. Progress. 22 (5), 1388–1393.

Kilian, K.A., Lai, L.M.H., Magenau, A., Cartland, S., Boecking, T., Di Girolamo, N., Gal, M., Gaus, K., Gooding, J.J., 2009. Smart tissue culture: in situ monitoring of the activity of protease enzymes secreted from live cells using nanostructured photonic crystals. Nano Lett. 9 (5), 2021–2025.

Kim, D.-N., Park, J., Koh, W.-G., 2009. Control of cell adhesion on poly(ethylene glycol) hydrogel surfaces using photochemical modification and micropatterning techniques. J. Ind. Eng. Chem. 15 (1), 124–128.

Koh, W.-G., Revzin, A., Pishko, M.V., 2002. Poly(ethylene glycol) hydrogel microstructures encapsulating living cells. Langmuir 1818 (7), 2459–2462.

Lamponi, S., Di Canio, C., Barbucci, R., 2009. Heterotypic cell-cell interaction on micropatterned surfaces. Int J. Artif. Organs 32 (8), 507–516.

Lee, H.J., Kim, D.N., Park, S., Lee, Y., Koh, W.G., 2011. Micropatterning of a nanoporous alumina membrane with poly(ethylene glycol) hydrogel to create cellular micropatterns on nanotopographic substrates. Acta Biomater. 7 (3), 1281–1289.

Low, S.P., Voelcker, N.H., Canham, L.T., Williams, K.A., 2009. The biocompatibility of porous silicon in tissues of the eye. Biomaterials 30 (15), 2873–2880.

Low, S.P., Williams, K.A., Canham, L.T., Voelcker, N.H., 2006. Evaluation of mammalian cell adhesion on surface-modified porous silicon. Biomaterials 27 (26), 4538–4546.

Parker, S.G., Yang, Y., Ciampi, S., Gupta, B., Kimpton, K., Mansfeld, F.M., Kavallaris, M., Gaus, K., Gooding, J.J., 2018. A photoelectrochemical platform for the capture and release of rare single cells. Nat. Commun. 9, 2288.

Raghavan, S., Chen, C.S., 2004. Micropatterned environments in cell biology. Adv. Mater. 16 (15), 1303–1313.

Revzin, A., Tompkins, R.G., Toner, M., 2003. Surface engineering with poly(ethylene glycol) photolithography to create high-density cell arrays on glass. Langmuir 19 (23), 9855–9862.

Revzin, R.J.R. Alexander, Yadavalli, Vamsi K., Koh, Won-Gun, Curt Deister, D.D.H., Mellott, Michael B., Pishko*, Michael V., 2001. Fabrication of poly(ethylene glycol) hydrogel microstructures using photolithography. Langmuir 17, 5440–5447.

Ruoslahti, E., 1996. RGD and other recognition sequences for integrins. Annu Rev. Cell Dev. Biol. 12, 697–715.

Ruoslahti, E., Pierschbacher, M., 1987. New perspectives in cell adhesion: RGD and integrins. Science 238 (4826), 491–497.

Schwartz, M.P., Derfus, A.M., Alvarez, S.D., Bhatia, S.N., Sailor, M.J., 2006. The smart petri dish: a nanostructured photonic crystal for real-time monitoring of living cells. Langmuir 22 (16), 7084–7090.

Shin, D.-S., Liu, Y., Gao, Y., Kwa, T., Matharu, Z., Revzin, A., 2012. Micropatterned surfaces functionalized with electroactive peptides for detecting protease release from cells. Anal. Chem. 85 (1), 220–227.

Shin, D.-S., Seo, J.H., Sutcliffe, J.L., Revzin, A., 2011. Photolabile micropatterned surfaces for cell capture and release. Chem. Commun. 47 (43), 11942–11944.

Shin, D.-S., You, J., Rahimian, A., Vu, T., Siltanen, C., Ehsanipour, A., Stybayeva, G., Sutcliffe, J., Revzin, A., 2014. Photodegradable hydrogels for capture, detection, and

release of live cells. Angew. Chem. (Int. Ed. Engl.) 53 (31), 8221–8224.
Son, K.J., Shin, D.S., Kwa, T., Gao, Y., Revzin, A., 2013. Micropatterned sensing hydrogels integrated with reconfigurable microfluidics for detecting protease release from cells. Anal. Chem. 85 (24), 11893–11901.
Sweetman, M.J., Ronci, M., Ghaemi, S.R., Craig, J.E., Voelcker, N.H., 2012. Porous silicon films micropatterned with bioelements as supports for mammalian cells. Adv. Funct. Mater. 22 (6), 1158–1166.
Sweetman, M.J., Shearer, C.J., Shapter, J.G., Voelcker, N.H., 2011. Dual silane surface functionalization for the selective attachment of human neuronal cells to porous silicon. Langmuir 27 (15), 9497–9503.
Tan, G., Wang, Y., Li, J., Zhang, S., 2008. Synthesis and characterization of injectable photocrosslinking poly(ethylene glycol) diacrylate based hydrogels. Polym. Bull. 61 (1), 91–98.
Yan, J., Revzin, A., 2012. Micropatterned biosensing surfaces for detection of cell-secreted inflammatory signals. Biosensors and molecular technologies for cancer diagnostics. Taylor & Francis, pp. 389–404.
Yan, J., Sun, Y., Zhu, H., Marcu, L., Revzin, A., 2009. Enzyme-containing hydrogel micropatterns serving a dual purpose of cell sequestration and metabolite detection. Biosens. Bioelectron. 24 (8), 2604–2610.
Yanagawa, F., Sugiura, S., Kanamori, T., 2016. Hydrogel microfabrication technology toward three dimensional tissue engineering. Regen. Ther. 3, 45–57.
Yap, F.L., Zhang, Y., 2007. Protein and cell micropatterning and its integration with micro/nanoparticles assembly. Biosens. Bioelectron. 22 (6), 775–788.
Yarmush, M.L., King, K.R., 2009. Living-cell microarrays. Annu. Rev. Biomed. Eng. 11, 235–257.
Yeh, C.-C., Venault, A., Chang, Y., 2016. Structural effect of poly(ethylene glycol) segmental length on biofouling and hemocompatibility. Polym. J. 48 (4), 551–558.
Zhang, S., Yan, L., Altman, M., Lassle, M., Nugent, H., Frankel, F., Lauffenburger, D.A., Whitesides, G.M., Rich, A., 1999. Biological surface engineering: a simple system for cell pattern formation. Biomaterials 20 (13), 1213–1220.
Zhu, H., Stybayeva, G., Macal, M., Ramanculov, E., George, M.D., Dandekar, S., Revzin, A., 2008. A microdevice for multiplexed detection of T-cell-secreted cytokines. Lab a Chip 8 (12), 2197–2205.
Zhu, H., Stybayeva, G., Silangcruz, J., Yan, J., Ramanculov, E., Satya, D., George, M., Revzin, A., 2009. Detecting cytokine release from single human T-cells. Anal. Chem. 81 (19), 8150–8156.